Contemporary Mathematics

Boundary Conditions for Fully Implicit Two-Phase Flow Models

Małgorzata Peszyńska, Eleanor W. Jenkins, and Mary F. Wheeler

Abstract. This paper describes a methodology for treating general boundary conditions for the fully implicit expanded mixed finite element method for modeling multi-phase flow in porous media. This approach, which is locally conservative, is useful for modeling multi-physics and multi-numerics in energy and environmental applications. Numerical experiments for two-phase flow are included.

1. Introduction

The contamination of groundwater is one of the most serious environmental problems facing the nation. For example, in 1996, the Department of Energy listed 10,000 Superfund sites, where groundwater contamination poses a serious threat to human health. The characterization and remediation of contaminated sites is difficult and expensive and only now is technology emerging to cope with this severe and widespread problem. Computation and modeling of multi-phase flow in permeable media plays a central role in these technologies and is essential for risk assessment, cost reduction, and the rational and efficient use of resources. Indeed, recent advances in computer hardware, software, and algorithms have established computation as a third pillar of science, joining theory and experiment. The mathematical formulations discussed here apply to both environmental remediation and to problems associated with the environmentally prudent production of hydrocarbon energy from existing oil and gas fields.

1991 *Mathematics Subject Classification.* Primary 65M60; Secondary 65M05,76S05,76T05.

Key words and phrases. two-phase flow, boundary conditions, implicit, finite elements, finite differences, expanded mixed method.

This work was partially supported by DOE grant DE-FG03-99ER25371, DOD grant PET2/ UTA01-347, and the NSF grants SBR 9873326, ITR EIA-0121523, and NPACI 10181410.

©0000 (copyright holder)

The central challenge in addressing these porous media problems is to maximize economic benefit from a resource whose properties are only poorly known and in which a variety of complex chemical and physical phenomena take place. The major tool of these efforts is a computational portal comprised of coupled programs that together account for multi-component, multi-phase flow and transport through heterogeneous geological structures. The coupled programs must accomodate different physical processess occurring simultaneously in different parts of the domain and, for computational efficiency, should also accommodate multiple numerical schemes. To accomplish this, researchers at the Center for Subsurface Modeling (CSM) at The University of Texas have developed a framework or problem solving environment which is called IPARS (**I**ntegrated **P**arallel **A**ccurrate **R**eservoir **S**imulator) [**PWP+97, WYW+97, ABE+, MSA+99, LNW00, PLW99, PLW00, PWY**].

IPARS represents a new approach to simulator development, emphasizing modularity of code, portability to many platforms, and ease of integration with other software. A key feature of the IPARS framework is that it allows for the mathematically rigorous treatment of multiple domains in which different physical processes are occurring, as well as providing a basis for implementing different numerical schemes in different parts of the domain. The near optimal scalability of IPARS is demonstrated in [**WPGED00**]. This software is being used by CSM collaborators in academia and in governmental and industrial laboratories.

A methodology for treating multi-physics and multi-numerical methods requires general boundary conditions, in particular for mortar multiblock [**ACWY00, Yot96**] and multi-model [**WAB+99, LPW01, PLW00, WWP00, Lu00**]. There is an extensive literature for well–posedness and regularity for general boundary conditions for general second order elliptic operators of which incompressible single–phase flow is an example. In addition, the formulation and analysis of Dirichlet, Robin, and Neumann conditions in mixed and expanded mixed finite element approximations to these equations is discussed in [**AWY97, ADK+98**]. Several papers on the treatment of incompressible multi-phase flow include the work of [**AD85, AWZ96, Arb92, Che97, CQE00, CK01**]. This is not the case for compressible or slightly compressible multiple flowing phases such as described by the two-phase problem presented in this paper or the three-phase black-oil model.

The purpose of this paper is to provide a formulation for imposing general boundary conditions for implicit discretizations based on expanded mixed finite element approximations to two-phase slightly compressible flow. We denote by Ω the computational domain and by $\partial\Omega$ its boundary. Two types of boundary conditions are considered here: the flux (Neumann) conditions imposed on the part of the boundary $\Gamma_N \subseteq \partial\Omega$, with a special case of the no–flow boundary $\Gamma_0 \subseteq \Gamma_N$, and the prescribed data (Dirichlet) conditions imposed on $\Gamma_D \subseteq \partial\Omega$. We assume that $\Gamma_N \cap \Gamma_D = \emptyset$ and that

$\overline{\Gamma_N} \cup \overline{\Gamma_D} = \overline{\partial\Omega}$. Other conditions are possible. For example, specification of one phase pressure and one component flux may be convenient. However, these extensions will not be discussed here.

In applications, the type and values of the boundary conditions may change in time. For example, in air/water problems the water table can periodically rise or fall on the boundary of an aquifer. Here we allow Γ_D, Γ_N, and the associated boundary values to change in time. The methodology described is computationally efficient and straightforward to implement. In our approach, one need only track and identify as a function of time those boundary faces that change type or value and compute corresponding transmissibilities. Numerical experiments are included in this paper to illustrate the soundness of this methodology.

The outline of the paper is as follows: In Section 2, we briefly describe the physical models. In Section 3, we define the expanded mixed finite element discretizations. In Section 4, general boundary conditions for these discretizations are formulated. Numerical examples are presented in Section 5 and conclusions are given in Section 6.

2. Model Formulation

The flow system is formulated as a continuity, or mass balance, equation, Darcy's Law modified for multi-phase flow, equation of state relationships describing the density of each fluid, capillary pressure relationships between two fluid interfaces, and a saturation relationship.

The mass balance equation for each of the α fluid phases is given by

$$\phi \frac{\partial N_\alpha}{\partial t} + \nabla \cdot \boldsymbol{U}_\alpha = q_\alpha, \tag{1}$$

where N_α is the concentration of the α phase, P_α is the pressure of the α phase, and q_α is a source term. The concentration is the product of the saturation and density, so that $N_\alpha = S_\alpha \rho_\alpha$. In the general two-phase flow model, α is either a wetting phase fluid, w, or a non-wetting phase fluid, n. We consider water as the wetting phase fluid, and either oil or air/gas as the non-wetting phase fluid.

Darcy's law for multi-phase flow is used to define the mass flux $\boldsymbol{U}_\alpha$ as

$$\boldsymbol{U}_\alpha = -\rho_\alpha K \frac{k_\alpha}{\mu_\alpha} \left(\nabla P_\alpha - \rho_\alpha G \nabla D \right). \tag{2}$$

Here, K is the permeability tensor, k_α is the relative permeability, μ_α is the viscosity, ρ_α is the density, G is gravity constant, and $D = D(x)$ is the depth of the reservoir. We will also use phase mobility $\lambda_\alpha =: \rho_\alpha \frac{k_\alpha}{\mu_\alpha}$ and phase potential defined by

$$\nabla \Psi_\alpha =: \nabla P_\alpha - \rho_\alpha G \nabla D \tag{3}$$

so that the Darcy equation may be rewritten as

$$\boldsymbol{U}_\alpha = -K \lambda_\alpha \nabla \Psi_\alpha. \tag{4}$$

Substituting the Darcy velocity into the mass balance equation (1) gives the governing equation for multi-phase flow

$$\phi \frac{\partial N_\alpha}{\partial t} - \nabla \cdot (\rho_\alpha K \frac{k_\alpha}{\mu_\alpha}(\nabla P_\alpha - \rho_\alpha g \nabla D)) = q_\alpha. \tag{5}$$

The system is closed using the saturation and capillary pressure relationships. The saturation relationship (or volume balance) is given as

$$\sum_\alpha S_\alpha = 1. \tag{6}$$

Capillary pressure is the difference in pressure across the interface between the non-wetting and wetting phase fluids which is a known function of saturation, so that

$$P_c(S_w) = P_n - P_w. \tag{7}$$

Examples of permeability and capillary pressure curves are given in Figure 2, which shows the respective degeneracies of these relationships.

Both water and oil phases are assumed to be slightly compressible, so that their densities are given by

$$\rho_\alpha = \rho_{\alpha,ref} \exp(c_\alpha P_\alpha), \quad \alpha = w, o \tag{8}$$

where c_α is the compressibility constant for the fluid and $\rho_{\alpha,ref}$ is a reference density. The density for the air phase is given by the real gas law,

$$\rho_a = \frac{P_a M}{Z(P_a) R T}, \quad \alpha = a \tag{9}$$

where M is the molecular weight, R is the gas constant, T is the temperature, and $Z(P_a)$ is a function of air pressure.

Finally, the initial condition of the reservoir needs to be defined. This can be done using an assumption of hydrostatic equilibrium or using *ad-hoc* values of primary unknowns. Here we will assume that the values of all phase pressures, saturations, and concentrations are known at time zero.

Weak formulation. We consider the spaces

$$(W, \boldsymbol{V}) = (L^2(\Omega), H(div; \Omega))$$

as well as the space $\Lambda \subset H^{\frac{1}{2}}(\partial\Omega)$ or $\Lambda \subset L^2(\partial\Omega)$. The first two spaces provide test functions and pressure and velocity variables, respectively, while the latter is used to define boundary values. The brackets $(\cdot, \cdot)$ will denote the inner product in W.

Using the spaces W, V, Λ, we obtain the weak form of (1) and (2). First we multiply (1) by a test function $w \in W$ and integrate over Ω as follows:

$$(\phi \frac{\partial N_\alpha}{\partial t}, w) + (\nabla \cdot \boldsymbol{U}_\alpha) = (q_\alpha, w), \quad \forall w \in W, \forall \alpha.$$

The weak form of (2) follows analogously except that the gradient of potential needs to be removed using integration by parts. We explain in detail how this is done in Section 3 when deriving variants of spatially discrete

equivalents of Darcy's equation (2) with the *expanded mixed method*. One approach is to introduce the variable $\tilde{\boldsymbol{U}}_\alpha$. We have

$$\begin{aligned}(\boldsymbol{U}_\alpha, \hat{\boldsymbol{v}}) &= (\lambda_\alpha \tilde{\boldsymbol{U}}_\alpha, \hat{\boldsymbol{v}}), \quad \forall\, \hat{\boldsymbol{v}} \in V, \forall \alpha, \\ \left(K^{-1}\tilde{\boldsymbol{U}}_\alpha, \boldsymbol{v}\right) &= (\Psi_\alpha, \nabla \cdot \boldsymbol{v}) - \int_{\partial\Omega} \Psi_\alpha\, \boldsymbol{v} \cdot \eta \, ds, \quad \forall \boldsymbol{v} \in V \text{ and } \forall \alpha.\end{aligned}$$

The treatment of different boundary conditions, which is the main topic of this paper, is apparent through the last term in the above equation. If only no–flow boundary conditions are imposed then the boundary term is zero since $\boldsymbol{v} \cdot \eta = 0$. Otherwise, while values of Ψ are defined directly or indirectly on Γ_D, they are replaced in the integral over Γ_N by Lagrange multipliers from the space Λ. An additional equation which guarantees the equality of fluxes with the prescribed Neumman data is imposed using test functions from Λ (see details in Section 4).

3. Spatial and Temporal Discretization

The model equations are discretized through the use of a cell–centered finite difference scheme which is equivalent to the expanded mixed finite element method where the approximation spaces are lowest order Raviart-Thomas spaces $(W_h, \boldsymbol{V}_h) \subset (W, \boldsymbol{V})$ on a rectangular grid. This follows the procedure described in [**RW83**] and outlined below. In this section we will only be concerned with interior equations or with test functions whose support is disjoint from $\partial\Omega$.

The functions in W_h are piecewise constant on each cell; a test function $w_{ijk} \in W_h$ is a characteristic function of the cell Ω_{ijk}. On the other hand, functions $\boldsymbol{v} \in \boldsymbol{V}_h$ are linear in one coordinate direction and constant in the others. We will frequently use the function $\boldsymbol{v} = \boldsymbol{v}_{i+1/2,jk}$ which is linear in x direction and constant in y, z directions and whose support is $\Omega_{ijk} \cup \Omega_{i+1,jk}$, and which has nodal value $v_{i+1/2,jk} = 1$. The scalar unknowns pressures (P_α), concentrations (N_α), and saturations (S_α), as well as the densities ρ_α, are interpreted as members of W_h. The vector unknown velocities $\boldsymbol{U}_\alpha$ are interpreted as members of $\boldsymbol{V}_h$. We will supress the subscript h in the following sections.

3.1. Spatial discretization. For every cell Ω_{ijk}, we denote its measure by V_{ijk}, and we compute its pore volume $\xi_{ijk} = V_{ijk}\phi_{ijk}$ where ϕ_{ijk} is the porosity of the cell. Note that if porosity is not changing as a function of time or pressure, then the pore volume is constant.

To discretize Equation (1), we multiply it by the test function w_{ijk} and integrate over Ω to get

$$\mathcal{A}_{\alpha,ijk} + \mathcal{T}_{\alpha,ijk} + \mathcal{W}_{\alpha,ijk} = 0, \tag{10}$$

where the accumulation $\mathcal{A}_{\alpha,ijk}$, transport $\mathcal{T}_{\alpha,ijk}$ and well $\mathcal{W}_{\alpha,ijk}$ terms come from respective terms in Equation (1) and are defined as follows:

$$\mathcal{A}_{\alpha,ijk} =: V_{ijk}\phi_{ijk}\frac{\partial N_\alpha}{\partial t} = \xi_{ijk}\frac{\partial N_\alpha}{\partial t}, \tag{11}$$

$$\mathcal{W}_{ijk} =: -\int_\Omega q_\alpha w_{ijk}\, dx = \int_{\Omega_{ijk}} q_\alpha\, dx. \tag{12}$$

Note that the well terms are non–zero only in cells which contain wells. In IPARS we define the well terms using the Peaceman formulation [**Pea83**].

The transport contribution is evaluated as

$$\mathcal{T}_{\alpha,ijk} \quad =: \quad \int_\Omega \nabla\cdot \boldsymbol{U}_\alpha w_{i,j,k} dx = \int_{\Omega_{i,j,k}} \nabla\cdot \boldsymbol{U}_\alpha dx.$$

For transport in the x direction we use the divergence theorem to obtain

$$\begin{aligned}\mathcal{T}^{x+}_{\alpha,ijk} + \mathcal{T}^{x-}_{\alpha,ijk} \quad &=: \quad \int_{\partial\Omega_{i+1/2,jk}} \boldsymbol{U}_{\alpha,i+1/2,jk}\cdot\nu dx + \int_{\partial\Omega_{i-1/2,jk}} \boldsymbol{U}_{\alpha,i-1/2,jk}\cdot\nu dx \\ &= \quad \triangle y_j \triangle z_k(\boldsymbol{U}_{\alpha,i+1/2,jk} - \boldsymbol{U}_{\alpha,i-1/2,jk}),\end{aligned}$$

where $\partial\Omega_{i+1/2,jk}$ is the $x+$ part of $\partial\Omega_{ijk}$. Terms in the y,z direction can be computed analogously and need to be added to $\mathcal{T}_{\alpha,ijk}$. The discrete velocity values $\boldsymbol{U}_{\alpha,i+1/2,jk}$ are defined below.

Discretization of Darcy's law. The discretization of Equation (2) is delicate as it must result in a locally conservative scheme as well as it must allow for discontinuity and for degeneracy of fluid–rock properties, specifically, of permeability K and of relative permeabilities k_α. We use the *expanded mixed method* which satisfies these conditions and which has optimal convergence properties [**AWY96, AWY97, ADK$^+$98**]. Moreover, if appropriate quadratures are used, it can be shown that this method gives a stencil equivalent to a cell–centered finite difference scheme (CCFD) [**RW83, AWY97, AWY96**].

Since discretization of velocities is more relevant to the topic of this paper, we review some of the related details and for the sake of brevity consider the $x+$ direction only. Extensions to other directions are straightforward for diagonal tensors. We do not elaborate on the full tensor case here.

First we follow [**RW83**] and consider the quantity $\boldsymbol{u}$ defined as

$$\boldsymbol{u} = -K\nabla P, \tag{13}$$

which can be thought of as single phase Darcy velocity with the viscosity μ lumped with K and with no gravity so that $\Psi = P$. If K is not degenerate then we can write $K^{-1}\boldsymbol{u} = -\nabla P$. This equation, when multiplied by $\boldsymbol{v} = \boldsymbol{v}_{i+1/2,jk} \in V_h$ and integrated over the support of $\boldsymbol{v}_{i+1/2,jk}$ with the trapezoidal rule applied to integration in the x direction and the midpoint rule applied in the y,z directions, yields the following finite difference

equation for the nodal value $u_{i+1/2,jk}$ of $\boldsymbol{u}$

$$\triangle y_j \triangle z_k \left(\frac{1}{2} \triangle x_i K^{-1}_{ijk} + \frac{1}{2} \triangle x_{i+1} K^{-1}_{i+1,jk} \right) u_{i+1/2,jk} = \triangle y_j \triangle z_k (P_{i+1,jk} - P_{ijk}) \tag{14}$$

Analogous equations in other directons can be written. Now define transmissibilities $T_{i+1/2,jk}$ as

$$T_{i+1/2,jk} = \triangle y_j \triangle z_k \left(\frac{1}{2} \triangle x_i K^{-1}_{ijk} + \frac{1}{2} \triangle x_{i+1} K^{-1}_{i+1,jk} \right)^{-1}, \tag{15}$$

and rewrite Equation (14) as

$$\triangle y_j \triangle z_k u_{i+1/2,jk} = T_{i+1/2,jk} (P_{i+1,jk} - P_{ijk}). \tag{16}$$

Note that the use of K in the above calculation is consistent with harmonic averaging of K_i and K_{i+1}.

Now, in order to allow for degenerate K, we follow [**AWY97**] and define $\tilde{\boldsymbol{u}} = -\nabla P$, which gives $u = K\tilde{\boldsymbol{u}}$. This is done at the cost of introducing an extra variable $\tilde{U}$ which may, in practical calculations, be eliminated. For example, if we use trapezoidal and midpoint integration rules to combine $(\tilde{\boldsymbol{u}}, \boldsymbol{v})_{TM} = (P, \nabla \cdot \boldsymbol{v})$ and $(\boldsymbol{u}, \boldsymbol{v})_{TM} = (K\tilde{\boldsymbol{u}}, \boldsymbol{v})_T$ then the following discrete equations for the nodal values $u_{i+1/2,jk}$, $\tilde{u}_{i+1/2,jk}$ become

$$\triangle y_j \triangle z_k \left(\frac{1}{2} \triangle x_i + \frac{1}{2} \triangle x_{i+1} \right) \tilde{u}_{i+1/2,jk} = \triangle y_j \triangle z_k (P_{i+1,jk} - P_{ijk}),$$

$$\triangle y_j \triangle z_k \left(\frac{1}{2} \triangle x_i + \frac{1}{2} \triangle x_{i+1} \right) u_{i+1/2,jk} = \triangle y_j \triangle z_k \left(\frac{1}{2} \triangle x_i K_{ijk} + \frac{1}{2} \triangle x_{i+1} K_{i+1,jk} \right) \tilde{u}_{i+1/2,jk}.$$

We can eliminate $\tilde{u}_{i+1/2,jk}$ to get a relationship similar to the one in Equation (14). However, the resulting transmissibilities no longer have the interpretation of harmonic averages.

Gravity terms. To explain how the gravity terms are included, instead of using $\tilde{\boldsymbol{u}} = -\nabla P$ and $\boldsymbol{u} = -K\nabla P$ as was done above, we discuss now $\tilde{\boldsymbol{u}} = -\nabla \Psi$ and

$$\boldsymbol{u} = -K\nabla\Psi. \tag{17}$$

For simplicity, we consider only one phase and supress the phase subscript $_\alpha$. We need to define discrete values of the depth, the density, and the potential variables. While the latter two are unknowns of the problem and are functions of pressure, the depth D is really a continuous variable which is given as data of the problem. In practical applications, density is likely to be an affine function of position allowing for the computational domain to be dipped from the gravity direction. Here we discretize D element by

element with a simple CCFD formula, $D_h|_{\Omega_{ijk}} = D_{ijk}$, with D_{ijk} being the depth of the center of the cell Ω_{ijk}, which is convenient in implementation

The density ρ is a function of pressure P which is approximated by piecewise constant P_h and therefore over the support of $\boldsymbol{v}_{i+1/2,jk}$ the density values D_h are defined as

$$\rho_h(P_h) = \begin{cases} \rho(P_{ijk}) & \text{in } \Omega_{ijk}, \\ \rho(P_{i+1,jk}) & \text{in } \Omega_{i+1,jk}. \end{cases}.$$

Similarly, discrete potential values Ψ_h can be defined as piecewise constants and over the support of $\boldsymbol{v}_{i+1/2,jk}$ they are given by

$$\Psi_h = \begin{cases} P_{ijk} - P_{ref} - \int_{D_{ref}}^{D_{ijk}} \rho dx & \text{in } \Omega_{ijk} \\ P_{i+1,jk} - P_{ref} - \int_{D_{ref}}^{D_{i+1,jk}} \rho dx & \text{in } \Omega_{i+1,jk} \end{cases}$$

where D_{ref}, P_{ref} are the reference depth and pressure at which potential is zero.

Now consider the following calculation

$$\begin{aligned} (\Psi_h, \nabla\cdot\boldsymbol{v}) &= (P_h, \nabla\cdot\boldsymbol{v}) - g\left(\int_{D_{ref}}^{D_{ijk}} \rho_\alpha\, dx, \nabla\cdot\boldsymbol{v}\right)_{\Omega_{ijk}} \\ &- G\left(\int_{D_{ref}}^{D_{i+1,jk}} \rho_\alpha\, dx, \nabla\cdot\boldsymbol{v}\right)_{\Omega_{i+1,jk}} \\ &= (P_h, \nabla\cdot\boldsymbol{v}) - G\left(\int_{D_i}^{D_{i+1}} \rho_\alpha\, dx, |\nabla\cdot\boldsymbol{v}|\right)_{\Omega_{ijk}\cup\Omega_{i+1,jk}} \end{aligned}$$

where the reference terms cancel out. To evaluate the density integral we now apply the trapezoidal rule to $(\int_{D_i}^{D_{i+1}} \rho\, dx)$ and we have $(\int_{D_i}^{D_{i+1}} \rho\, dx)_T = \frac{1}{2}(\rho_{ijk} + \rho_{i+1,jk})(D_{i+1,jk} - D_{ijk})$. Define $\rho_{i+1/2} =: \frac{1}{2}(\rho_{ijk} + \rho_{i+1,jk})$, which is the average value of ρ over the cells Ω_{ijk} and $\Omega_{i+1,jk}$. The above calculation is then completed by

$$(\Psi_h, \nabla\cdot\boldsymbol{v}) = P_{i+1,jk} - P_{ijk} - G\rho_{i+1/2}(D_{i+1,jk} - D_{ijk}).$$

The discrete counterpart of Equation (17) is then analogous to Equation (14) as follows

$$\begin{aligned} (18)\qquad \triangle y_j \triangle z_k \left(\frac{1}{2}\triangle x_i K^{-1}_{ijk} + \frac{1}{2}\triangle x_{i+1} K^{-1}_{i+1,jk}\right) u_{i+1/2,jk} = \\ = \triangle y_j \triangle z_k (\Psi_{i+1,jk} - \Psi_{ijk}) \\ = \triangle y_j \triangle z_k (P_{i+1,jk} - P_{ijk}) - g\rho_{i+1/2}(D_{i+1,jk} - D_{ijk}) \end{aligned}$$

Mobilities in multi-phase Darcy's law. In the multi-phase flow case discussed in this paper we need to discretize Darcy's equation (2) in the form $\boldsymbol{U}_\alpha = -K\lambda_\alpha \nabla\Psi_\alpha = -K\rho_\alpha \frac{k_\alpha}{\mu_\alpha}\nabla\Psi_\alpha$ Here we also need to account for the dependence of mobilities λ_α upon the pressures and saturations and

for their possible degeneracy. We proceed with the product $K\lambda_\alpha$ in $\boldsymbol{U}_\alpha$ also using the expanded mixed method as was shown above for K in $\boldsymbol{u}$.

In fact, there are at least two ways of decomposing $\boldsymbol{U}_\alpha$. The first with $\boldsymbol{U}_\alpha = K\lambda_\alpha \tilde{\boldsymbol{U}}_\alpha$; $\tilde{\boldsymbol{U}}_\alpha = -\nabla\Psi_\alpha$ results in non–harmonic averaging of K but allows for degenerate K. The second, $\boldsymbol{U}_\alpha = \lambda_\alpha \tilde{\boldsymbol{U}}_\alpha$; $K^{-1}\tilde{\boldsymbol{U}}_\alpha = -\nabla\Psi_\alpha$, allows for degeneracy of the nonlinear terms λ_α but not of K and results in harmonically averaged permeabilities.

Regardless of the choice, the mobilities introduce a hyperbolic type nonlinearity which cannot be treated with symmetric differences. For stability we use upwinding, which is also known as one-point upstream weighting. Alternatives include new approaches based on Kirchoff transformations and higher order spline approximations [**Eat01**] or higher order upwinding. We define the discrete mobility as

$$\lambda_{\alpha,sjk} =: \frac{1}{\mu_\alpha} k_\alpha(S_{w,sjk})\rho_\alpha(P_{\alpha,sjk}), \tag{19}$$

with the s in sjk found by upwinding

$$s = \begin{cases} i & \text{if } P_{ijk} \geq P_{i+1,jk} \\ i+1 & \text{otherwise.} \end{cases} \tag{20}$$

In summary, the *expanded mixed method* or CCFD discretization of multi-phase Darcy's law (2) is, in the strict interior,

$$\begin{aligned} \triangle y_j \triangle z_k \boldsymbol{U}_{\alpha,i+1/2,jk} = T_{i+1/2,jk}\lambda_{\alpha,sjk}\big(P_{\alpha,i+1,jk} - P_{\alpha,ijk} \\ -G\rho_{i+1/2,jk}(D_{i+1,jk} - D_{ijk})\Big). \end{aligned} \tag{21}$$

In cells adjacent to the boundary we need to consider boundary conditions and appropriately modify the spaces $V_h \subset V$. This is discussed in Section 4 for general boundary conditions. However, in case of no-flow conditions we can simply set transmissibilities to zero on faces adjacent to the boundaries.

3.2. Backward Euler discretization in time. Several techniques have been used and analyzed for temporal integration of the equation (5), and these include implicit, IMPES (IMplicit Pressure Explicit Saturations), explicit and other methods [**AS79**]. In this paper we focus on a *fully implicit* method which arises from the backward Euler scheme. At time t_{n+1} we have from Equation (5)

$$\phi\frac{N_\alpha^{n+1} - N_\alpha^n}{\triangle t_{n+1}} - \nabla\cdot(K\frac{\rho_\alpha^{n+1}k_\alpha^{n+1}}{\mu_\alpha}(\nabla P_\alpha^{n+1} - \rho_\alpha^{n+1}G\nabla D)) = q_\alpha^{n+1}.$$

In order to obtain a fully discrete formulation, we apply the backward-Euler time discretization to the spatially discretized Equations (10) and (21) and we multiply them by the time step $\triangle t = \triangle t_{n+1}$. The fully discrete

implicit equation for a cell Ω_{ijk} is

$$\xi_{ijk}(N_\alpha^{n+1} - N_\alpha^n) - \triangle t \lambda_{\alpha,sjk}^{n+1} \Big(T_{i+1/2,jk} \left(\Psi_{i+1,jk}^{n+1} - \Psi_{ijk}^{n+1} \right) - T_{i-1/2,jk} \left(\Psi_{i,jk}^{n+1} - \Psi_{i-1,jk}^{n+1} \right) \Big) - \triangle t q_{ijk} = 0,$$

which can be written in residual form as

$$\mathcal{R}_{\alpha,ijk}^{n+1} = \mathcal{A}_{\alpha,ijk}^{n+1} + \mathcal{T}_{\alpha,ijk}^{n+1} + \mathcal{W}_{\alpha,ijk}^{n+1} = 0, \tag{22}$$

where the discrete–in–time residuals contain the term $\triangle t_{n+1}$ and otherwise are defined analogously to the continuous residuals. Equation (22) can be written also as

$$\begin{cases} \mathcal{R}_{o,ijk}^{n+1} = 0, & \forall i,j,k: \quad \text{nonwetting (oil) equation,} \\ \mathcal{R}_{w,ijk}^{n+1} = 0, & \forall i,j,k: \quad \text{wetting (water) equation,} \end{cases}$$

which is convenient when computing Jacobian entries (see Section 4).

We must solve the resulting nonlinear system

$$\mathcal{R}_{\alpha,ijk}^{n+1} = 0, \quad \forall i,j,k, \quad \forall \alpha = n, w$$

for the values of discrete *primary unknowns*. These can be chosen in several ways. Common choices include using pressure of one phase as one unknown and saturation or concentration of the same phase as the other primary unknown. As another example, the choice of two pressures, though it appears natural, may be inappropriate in cases where the derivative of capillary pressure is close to 0.

In our implementation in IPARS, the two-phase oil-water model uses oil pressure P_o and oil concentration N_o as primary unknowns, while the air-water model uses water pressure P_w and water saturation S_w. The values of primary unknowns at time $t = 0$ or for $n = 0$ are defined by the initial condition. The nonlinear residual equation (22) is solved using an inexact Newton method, where the Newton step is solved using GMRES with sophisticated two-stage and multigrid preconditioners [**DKWW97, Edw98, LVW**].

Jacobian calculations are based on a *7–point stencil*, which is the tightest stencil in 3 dimensions appropriate for diagonal tensor permeabilities. Our Jacobian is computed analytically but it is not exact as we often choose to drop lower order terms. This does not harm the convergence properties of the method and allows for faster construction of the Jacobian as some of the lower order terms can be computationally expensive. For example, in the two-phase oil-water model the dependence of water density on pressure is often ignored as this derivative is scaled by a (water) compressibility constant, which is of the order of 10^{-7}.

4. Boundary Condition Contributions

In this section we define types of boundary conditions that can be imposed on the external boundary $\partial\Omega$ on solutions to the problem described by Equation (5) and which, after discretization, are applied to each element

adjacent to the external boundary of Ω. We also define contributions to the residual and Jacobian of the nonlinear system in (22) from boundary terms.

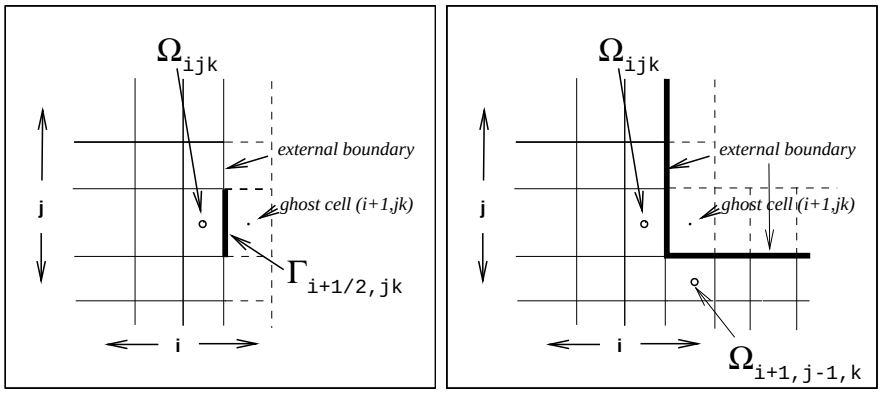

FIGURE 1. Computational domain with interior and boundary cells. Straight (left) and angular (right) boundary.

Geometry and notation. In the discussion below we will assume that the computational domain has a geometry similar to the ijk grid shown in Figure 1. More complicated geometries can be handled easily. In general, boundary faces and relevant values will be denoted by subscript $_L$ and also by superscript *. We have $\partial\Omega = \bigcup_L \Gamma_L$. Consider a cell $\Omega_{ijk} \subset \Omega$. The $x-$ and $x+$ neighbors of the cell Ω_{ijk} are cells $\Omega_{i-1,jk}$ and $\Omega_{i+1,jk}$ with faces between these cells denoted by $\partial\Omega_{i-1/2,jk}$ and $\partial\Omega_{i+1/2,jk}$, respectively. Suppose that $\partial\Omega_{ijk} \cap \partial\Omega \neq \emptyset$ and in particular that the edge (face) $\partial\Omega_{i+1/2,jk} \subset \partial\Omega$ as in Figure 1. This face $\partial\Omega_{i+1/2,jk}$ will be denoted by $\Gamma_{i+1/2,jk}$ or Γ_L. For convenience in implementation one can assume that $\Omega_{i+1,jk}$ which is called a "ghost cell", provides storage for the boundary values and for related calculations. Note that $\Omega_{i+1,jk}$ is a ghost cell for both Ω_{ijk} and for $\Omega_{i+1,j-1,k}$ in the case of an angular boundary, which requires care in implementation. In general, extending the computational domain by adding "ghost cells" does not substantially increase memory requirements. Of course, other implementation solutions are possible.

We will assume that each Γ_L can be in at most one of the two sets Γ_D, Γ_N. In other words, at most one of the conditions can be applied on a given face of a cell and at most one set of relevant values of fluxes or of Dirichlet data can be applied. In applications, this condition can be easily removed in the case of Dirichlet or of non–homogeneous flux conditions imposed on a portion of a face where the remaining part is considered to be a no-flow boundary. In implementation, such a condition can be reflected by including the area of only the "active" part of the cell in the transmissibilities across the face by generalizing the calculations presented below. This extension may be desired for the user's convenience but as it is less rigorous will not be considered here.

4.1. Discrete form of boundary conditions. The discrete equations discussed in Section 3 were valid in the strict interior, i.e., for cells Ω_{ijk} such that $\partial\Omega \cap \Omega_{ijk} = \emptyset$. Now we proceed to discuss the discretization of boundary terms. We first discuss a simple model problem with a simple form of Darcy's law as in Equation (13) and follow with its multi-phase extension (2).

Consider the following problem

$$\boldsymbol{u} = -K\nabla P \tag{23}$$

$$P|_{\Gamma_D} = P^* \tag{24}$$

$$\boldsymbol{u}\cdot\eta|_{\Gamma_N} = \boldsymbol{u}^* \tag{25}$$

where $P^* \in \Lambda$, $\boldsymbol{u}^* \in \Lambda \times \Lambda$ are given. We use the the discrete subset $\Lambda_h \subset \Lambda$ and drop the subscript $_h$ as before. The weak form of (23) is as follows: find $(\boldsymbol{u}, \lambda) \in (V, \Lambda)$ such that

$$\begin{aligned}
(K^{-1}\boldsymbol{u}, \boldsymbol{v}) &= (P, \nabla\cdot\boldsymbol{v}) - \int_{\Gamma_D} P\boldsymbol{v}\cdot\eta\, d\gamma - \int_{\Gamma_N} \lambda\boldsymbol{v}\cdot\eta\, d\gamma, \quad \forall \boldsymbol{v} \in V \\
\int_{\Gamma_N} \boldsymbol{u}\cdot\eta\xi\, d\gamma &= \int_{\Gamma_N} \boldsymbol{u}^*\xi\, d\gamma, \quad \forall \xi \in \Lambda,
\end{aligned}$$

where these equations are complemented by a weak form of some appropriate mass conservation equation analogous to (1) and the whole systems is solved for $(P, \boldsymbol{u}, \lambda) \in (W, V, \Lambda)$. Now we calculate the discrete transport across $\Gamma_{i+1/2,jk} \equiv \Gamma_L$, which is nothing else than a counterpart of Equation (14) across the boundary. Since we assumed that Γ_L can be at most in one of Γ_D or Γ_N, we need to consider each of the cases separately. The integrals with $\boldsymbol{u}$ are computed using the trapezoidal rule in x and the midpoint rule in y, z, and we get

$$\text{if } \Gamma_L \cap \Gamma_D = \Gamma_L \quad : \quad \triangle y_j \triangle z_k \left(\frac{1}{2} \triangle x_i K_{ijk}^{-1}\right) u_{i+1/2,jk} = \triangle y_j \triangle z_k (P_L^* - P_{ijk})$$

$$\text{if } \Gamma_L \cap \Gamma_N = \Gamma_L \quad : \quad \begin{cases} \triangle y_j \triangle z_k \left(\frac{1}{2} \triangle x_i K_{ijk}^{-1}\right) u_{i+1/2,jk} & = \triangle y_j \triangle z_k (\lambda_L - P_{ijk}) \\ \triangle y_j \triangle z_k u_{i+1/2,jk} & = \triangle y_j \triangle z_k u_L^* \end{cases}.$$

The above result was obtained with the standard mixed method. The expanded mixed method leads to the same discrete result. Note that the unknown Lagrange multiplier λ_L can be easily eliminated using u_L^*.

The above form suggests using a "transmissibility on the boundary" T_L as a counterpart of $T_{i+1/2,jk}$ as defined by (15)

$$T_L =: \triangle y_j \triangle z_k (\triangle x_i / 2K_{ijk})^{-1}$$

which, for a homogeneous permeability field and a uniform grid, is twice the size of the interior transmissibility $T_{i+1/2,jk}$. Transmissibilities defined this way help to unify the notation for interior and boundary transport.

The definitions above also cover the case of a no-flow boundary where for certain elements L we have $\Gamma_L \cap \Gamma_0 = \Gamma_L$. This can be easily handled

in implementation by setting $T_L = 0$ or by using $\boldsymbol{u}_L^* = 0$. Of course, it may also happen that $\partial\Omega = \Gamma_0$.

Multi-phase Darcy's law. For multi-phase Darcy's law (2) we specify values

$$\boldsymbol{U}_\alpha = -K\lambda_\alpha \nabla\Psi_\alpha, \quad \forall\alpha \tag{26}$$

$$\Xi_m|_{\Gamma_D} = \Xi_m^* \quad \text{for } m = 1,2 \tag{27}$$

$$\boldsymbol{U}_\alpha \cdot \eta|_{\Gamma_N} = \mathcal{U}_\alpha^* \quad \forall\alpha. \tag{28}$$

In the above equation, we used $\Xi_m, m = 1,2 \in \Lambda$ to denote two (primary or not primary) unknowns whose values need to be specified. For example, we can choose $\Xi_1 = P_w$; $\Xi_2 = S_w$. Other choices, discretization, and implementation are described in detail in Section 4.3.

In the fully implicit model discussed in this paper, the transport contribution across $\Gamma_{i+1/2,jk} \equiv \Gamma_L$ has the discrete form

$$\mathcal{T}_{\alpha,ijk}^{x+} = \triangle t\, T_L \lambda_{\alpha,sjk}(\Psi_\alpha^* - \Psi_{\alpha,ijk}), \quad \alpha = w,n$$

where the $n+1$ superscript has been supressed. The residual contributions $\mathcal{T}_{ijk}^{x+}$ and related Jacobian entries depend on the type and specification of boundary condition involved. Note that the general formulation accounts for gravity and density terms.

In Section 4.2 we discuss the details of Neumann conditions and in Section 4.3 we discuss Dirichlet conditions.

4.2. Flux boundary conditions. A *natural* condition to be specified on the boundary $\partial\Omega$ is the Neumann-type condition in which the flux of the components or phases is prescribed. In the context of this paper the Neumann condition is called "natural" for two reasons. First, in multi-phase flow models used in oil reservoir simulations, the boundaries of computational domains are frequently defined by impermeable geological barriers whose position may not be known precisely. Such is also the case of air-water flow models in confined aquifers. Second, in the mixed formulation, as will be clear from the discussion below, it is natural to include the contribution from the flux.

The simplest case is the no–flow boundary condition in which we set

$$U_{\alpha,i+1/2,jk} \cdot \eta|_{\Gamma_L} = 0, \quad \forall\alpha.$$

In this case there are no contributions to either the Jacobian or to the residuals. In implementation, this can be easily accounted for by setting the transmissibility $T_L = 0$ at the boundary as mentioned above.

For other flux conditions, the discrete form of (28) is

$$U_{\alpha,i+1/2,jk} \cdot \eta|_{\Gamma_L} = \mathcal{U}_{L,\alpha}^*, \quad \forall\alpha$$

where $\mathcal{U}_{L,\alpha}^*$ is given. In this case there is a contribution to each of the residuals

$$\mathcal{T}_{\alpha,ijk}^{x+} \leftarrow \mathcal{U}_{L,\alpha}^* \Delta y_j \Delta z_k \ \triangle t, \quad \forall\alpha$$

but this condition does not affect the Jacobian.

4.3. Dirichlet conditions. In the Dirichlet condition (27) we allow for the values of the pressures or of other scalar unknowns to be prescribed on Γ_D. This condition is not natural for either the (expanded) mixed formulation or for cell–centered finite differences, but it is frequently used in test cases or in comparisons with analytical solutions. However, little has been proven, in general, about the well-posedness of such conditions. Also, special considerations must be given to the Dirichlet condition on the outflow boundary.

In general, the conditions may be imposed on primary unknowns of the nonlinear system or on some other unknowns. Applications may dictate what conditions are natural or useful. In particular, it may be more natural to impose conditions on Ψ_α than on P_α but for simplicity we will only discuss the conditions imposed on pressures.

For example, consider

$$P_\alpha|_{\Gamma_{i+1/2,jk}} = P^*_{\alpha,L}$$
$$S_\alpha|_{\Gamma_{i+1/2,jk}} = S^*_{\alpha,L}$$

for a fixed phase α (wetting or non-wetting). This is the easiest of the conditions because the values of any other variables can be computed in a straightforward manner using Equations (6),(7),(8) or (9). We will assume henceforth that any of the values are known on L.

Consider now the implications of this condition. From the definitions above we have

$$U_{\alpha,i+1/2,jk} = T_L \lambda_{\alpha,sjk}(\Psi^*_{\alpha,L} - \Psi_{\alpha,ijk}),$$

where the value of s is determined by upwinding. If the upwind value $s = *$ (flow of phase α goes into Ω), then the mobility value $\lambda_{\alpha,skj}$ is computed from the boundary value of water saturation S^*_w which is either given or can be computed from S^*_o as $S^*_w = 1 - S^*_o$. Density and potential values for phase α are similarly obtained. Otherwise, if $s = i$ (flow of phase α goes out of Ω), then it is natural to use the interior value $S_{w,ijk}$ which corresponds to the *outflow* condition. Users may choose to override it and then a boundary layer is introduced.

As another example, consider the condition

$$P_w|_{\Gamma_{i+1/2,jk}} = P^*_{w,L}$$
$$P_n|_{\Gamma_{i+1/2,jk}} = P^*_{n,L},$$

which at a first glance appears natural. However, several restrictions will apply. For example, the difference of pressure values $P^*_{n,L} - P^*_{w,L}$ should be in the range of capillary pressure relationships. Moreover, the direction of induced flow of one phase should agree with the flow of the other phase, except for rare cases when the opposite may be physically justified.

As a last example, one may wish to impose conditions on primary unknowns of the nonlinear system or on some other unknowns. The latter is often the case when coupling models.

For example, for the two-phase oil-water model whose primary unknowns are P_o, N_o we prescribe

$$P_w|_{\Gamma_{i+1/2,jk}} = P^*_{w,L},$$
$$N_o|_{\Gamma_{i+1/2,jk}} = N^*_{o,L}.$$

To handle this condition, we construct a map which delivers the values of all primary and auxiliary variables. In this case, we have to solve

$$N^*_o = \rho_o(P^*_o)S^*_o = \rho_o\left(P^*_w + P_c(S^*_w)\right)(1 - S^*_w)$$

by a local Newtonian iteration for S^*_w. Once S^*_w is known, all other values follow.

Jacobian and residual contributions. As we have seen, regardless of whether the conditions are defined for primary unknowns or whether they are defined for other than primary unknowns, it is necessary to compute all relevant properties on the boundary or in the interior of the cell adjacent to the boundary. Once this is done, it is not difficult to calculate contributions to the nonlinear system.

As an example of such contributions, we consider here the oil-water model with primary unknowns oil pressure P_o and oil concentration N_o. The contributions to each of the "equations" in (22) depend on the upwinding. We shall also drop all terms with compressibility. For example, we have that $S_w = 1 - \frac{N_o}{\rho_o(P_o)}$, so $\frac{\partial S_w}{\partial N_o} = \frac{1}{\rho_o}$ and we can approximate $\frac{\partial S_w}{\partial P_o} \approx 0$. Also, $\frac{\partial \rho_o}{\partial P_o} = c_o\rho_o \approx 0$ since c_w is small. Similar terms will be dropped for the water phase. For simplicity in the calculations above we will assume that $D_{ijk} = D_{i+1,jk}$ and thus we will omit all the gravity terms. Of course, the latter is not assumed in the implementation.

If $s = *$, then the contribution to the residual in the "oil equation" is

$$\mathcal{T}^{x+}_{o,ijk} = T_L\lambda^*_o\left(P^*_o - P_{o,ijk}\right).$$

Now we define the Jacobian entries using the approximations mentioned above. We have

$$\frac{\partial \mathcal{T}^{x+}_{o,ijk}}{\partial P_{o,ijk}} =: -T_L\lambda^*$$
$$\frac{\partial \mathcal{T}^{x+}_{o,ijk}}{\partial N_{o,ijk}} =: 0.$$

If $s = i$, then the mobility is determined using $S_{w,ijk}$ and we have the residual contribution

$$\mathcal{T}^{x+}_{o,ijk} = T_L\lambda_{o,ijk}\left(P^*_o - P_{o,ijk}\right),$$

and the contributions to the Jacobian are approximated by

$$\begin{aligned}\frac{\partial \mathcal{T}^{x+}_{o,ijk}}{\partial P_{o,ijk}} &=: -T_L \lambda_{o,ijk} \\ \frac{\partial \mathcal{T}^{x+}_{o,ijk}}{\partial N_{o,ijk}} &=: -T_L \frac{k'_{o,ijk}}{\mu_o} \left(P^* - P_{o,ijk}\right).\end{aligned}$$

The contributions to the Jacobian coming from the "water equation" are similar except that we now also use the capillary pressure relationship (7). The differentiation with respect to $P_{o,ijk}$ reveals that, regardless of upwinding, we can use

$$\frac{\partial \mathcal{T}^{x+}_{w,ijk}}{\partial P_{o,ijk}} =: -T_L \lambda_{w,sjk}.$$

For differentiation with respect to $N_{o,ijk}$, we have with $s = i$

$$\frac{\partial \mathcal{T}^{x+}_{w,ijk}}{\partial N_{o,ijk}} =: -T_L \left(k'_w(S_{w,ijk}) \frac{\rho_w}{\rho_o} \left(P^*_w - P_{w,ijk}\right) + \lambda_{w,ijk} P'_c\left(S_{w,ijk}\right) \frac{1}{\rho_o} \right),$$

and if $s = *$ we define

$$\frac{\partial \mathcal{T}^{x+}_{w,ijk}}{\partial N_{o,ijk}} =: -T_L \lambda^*_w P'_c\left(S_{w,ijk}\right) \frac{1}{\rho_o}.$$

We conclude this section by stating that the entries in the air-water model are, of course, different. In particular, treatment of compressibilities requires special attention.

5. Numerical Examples

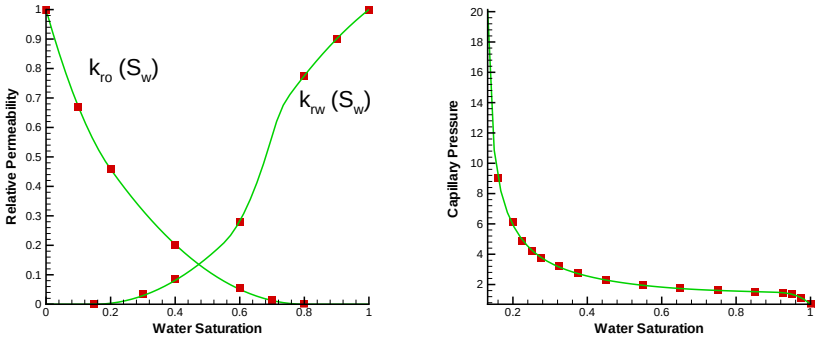

FIGURE 2. Relative permeability (left) and capillary pressure (right) as functions of wetting phase saturation

In this section we describe the numerical results for three test cases, which are, respectively, one-, two-, and three-dimensional.

In all numerical examples, we use the relative permeability-saturation relationship shown in Figure 2. All of the functional relationships are evaluted using a table lookup with piecewise splines, which handles the removal of singularities for capillary pressure [**IPA00, Whe**]. The latter capability is essential in handling capillary pressure data which typically has a pole at residual values of S_w (see Figure 2). We used this capillary pressure and permeability data in Examples 2 and 3.

All spatial dimensions given below are in $[ft]$ and all pressure values are given in $[psi]$. permeability units are in $[md]$. We used standard values for oil and water densities, viscosities and compressibilities except for Example 1 where we assumed incompresible fluids. We set the tolerance for the nonlinear solver to ensure that we receive mass balances correct to seven digits.

5.1. One–dimensional Buckley-Leverett problem. One of the motivations for implementing general boundary conditions into our framework was the need for comparison of our model with experimental data from core floods or with analytical solutions for multi-phase problems from the literature. The Buckley-Leverett problem [**BL42**] is a standard way of validating the results of two-phase, incompressible flow models. This problem describes the displacement of a nonwetting phase fluid by a wetting phase fluid in a one-dimensional, horizontal system with no capillary effects. The analytical solution can be constructed and compared to the numerical solution.

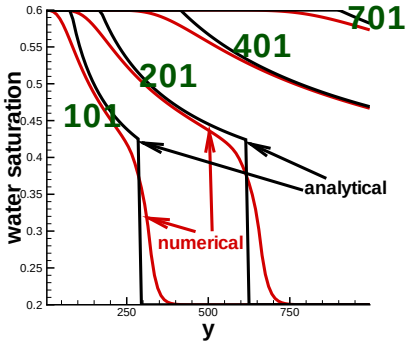

FIGURE 3. Comparison of analytical and numerical solutions for Buckley-Leverett problem

We simulate the Buckley-Leverett problem by imposing Dirichlet conditions at the horizontal ends of our reservoir. Our reservoir is $10 \times 1000 \times 10$, with permeability in y (horizontal) direction equal 500. We specify oil pressure of 550 and oil concentration of 0.6 at the left end of the reservoir, and oil pressure of 300 and water saturation of 0.4 at the right end. The reservoir was initialized at an oil pressure of 500 and water saturation 0.2.

Figure 3 shows a comparison between the numerical and analytical solutions to the Buckley-Leverett problem. The size of a mesh cell is $10 \times 10 \times 10$, and the time step size is 1 day. The curves in the figure show the solutions at 101, 201, 401 and 701 days.

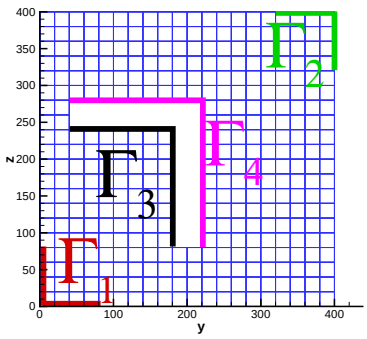

FIGURE 4. Two-dimensional case: grid and boundary regions

5.2. Two-Dimensional Example. In this example we demonstrate the use of several types of boundary conditions using a two-dimensional domain. The domain is a square 400x400 discretized with a 20x20 grid with uniform and isotropic permeability field with each of the entries of tensor $K = 200$. The flow is driven by boundary conditions imposed on Γ_1 and Γ_2 which are located in the lower left and upper right corners, respectively. Specifically, we impose

$$P_o|_{\Gamma_1} = 550$$
$$S_w|_{\Gamma_1} = 0.8$$

and we request that

$$P_o|_{\Gamma_2} = 300.$$

Saturation condition on Γ_2 may be imposed using the same saturation value as is used at initialization

$$S_w|_{\Gamma_2} = 0.2.$$

However, this condition will create boundary layer at time close to breakthrough. Instead, we use an outflow condition letting the flow cross Γ_2.

In the interior of the domain there is an L–shaped obstacle. Such structure can be modeled by using an internal boundary $\Gamma_{obstacle} = \Gamma_3 \cup \Gamma_4$ with elements belonging to the obstacle "keyed-out" of the computational domain, see Figure 4. Three different variants of boundary conditions imposed on $\Gamma_{obstacle}$ are considered and discussed below. In addition, $\bar{\partial\Omega} \setminus \left(\cup_{i=1}^{4} \bar{\Gamma}_i\right) = \bar{\Gamma}_0$.

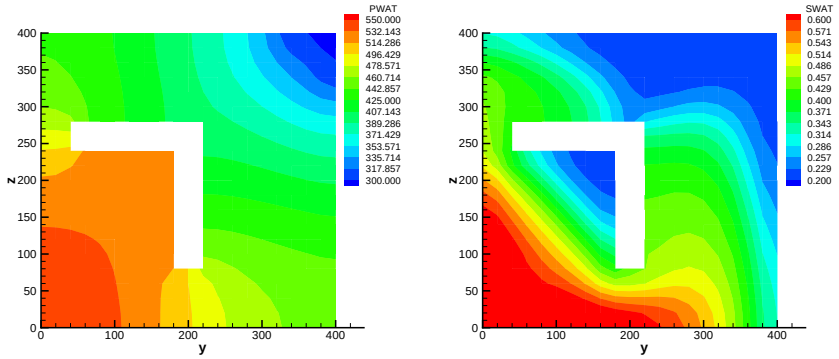

FIGURE 5. Two-dimensional case: profiles of P_w (left) and S_w (right) after 200 days. Boundary conditions in variant A.

A) In this case we assume that the region bounded by $\Gamma_{obstacle}$ is a very low permeability region or impermeable strata which provides an obstacle for the flow. Here we use the no-flow boundary condition on $\Gamma_{obstacle}$. Results are shown in Figure 5. Note that flow goes around the obstacle and that there are no gradients of pressure cross $\Gamma_{obstacle}$. As an alternative to "keyed-out" elements, one could use here very low permeability cells.

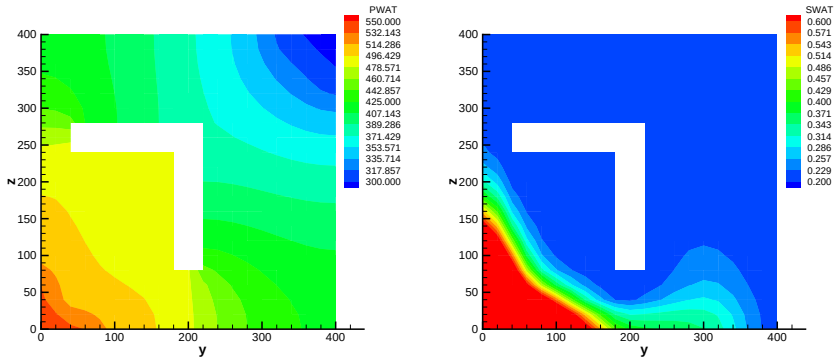

FIGURE 6. Two-dimensional case: profiles of P_w (left) and S_w (right) after 200 days. Boundary conditions in variant B.

B) In this example we allow for the upstream side of the strata Γ_3 to be permeable and we maintain a pressure condition to be $P_o^* = 500$ while we maintain a fixed saturation $S_w^* = .2$. We use no-flow condition on Γ_4. In applications, this case could correspond to a case where inside of the "obstacle" there is high content of non-wetting fluid which is being continuously replenished. Pressure and saturation profiles after 200 days are shown in Figure 6. In this example, a boundary layer arises.

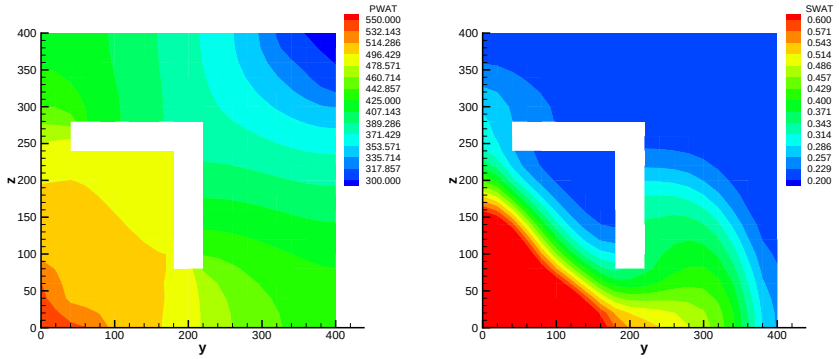

FIGURE 7. Two-dimensional case: profiles of P_w (left) and S_w (right) after 200 days. Boundary conditions in variant C.

C) This case is similar to B) except that, in order to prevent the boundary layer, we impose outflow condition with $P_o^* = 500$. In this way the interface Γ_3 becomes a seepage face through which we allow any flow to occur. See results in Figure 7: note the difference between those for case B and those for case C.

5.3. Three–dimensional field example: flow around a bend. This example demonstrates that our formulation and implementation in the IPARS framework allows full 3D complicated geometries as well as temporally dependent boundary conditions.

The computational domain covers a region of complicated lithology around an oxbow bend, with a 2^o angle away from the principal gravity direction. The grid is highly irregular (see Figure 8), and permeability layers are aligned with the grid. The permeabilities are heterogeneous; in the vertical direction, the permeability is 200 everywhere except layers 4 and 7 where it equals 30 and 40, respectively. It is also anisotropic: permeability in the vertical direction is 25, 5, and 3 in the respective layers. The reservoir is initially filled with water and the slightly compressible non–wetting fluid in hydrostatic equilibrium, with the non-wetting phase pressures on top of reservoir set to 600 and a water saturation of $S_w = 0.35$.

At the beginning of the simulation, we impose Dirichlet conditions on the non-wetting phase pressure and water saturation on boundaries Γ_1 and Γ_2, and Γ_3,

$$\begin{aligned} P_n|_{\Gamma_1} &= 650, \;\; S_w|_{\Gamma_1} = 0.7, \\ P_n|_{\Gamma_2} &= 650, \;\; S_w|_{\Gamma_2} = 0.7, \\ \text{and } P_n|_{\Gamma_3} &= 500, \;\; S_w|_{\Gamma_3} = 0.3. \end{aligned}$$

Thus water is initially introduced into the reservoir through Γ_1 and Γ_2, which can be seen in Figure 9. The boundary region Γ_4 is initially inactive.

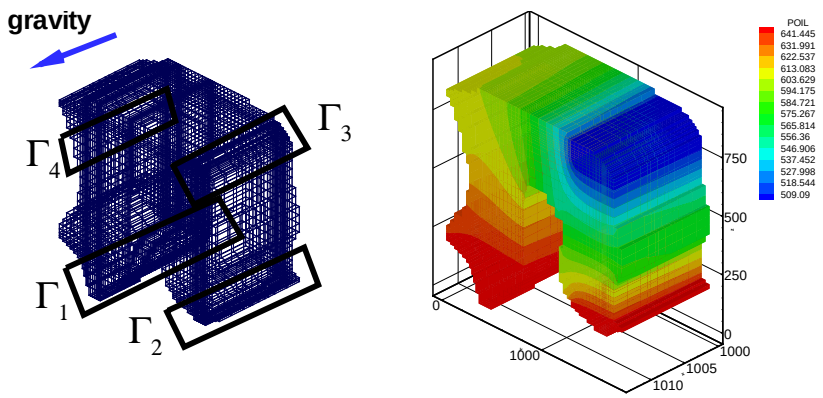

FIGURE 8. Mesh with boundary condition regions and non-wetting phase pressure at day 1

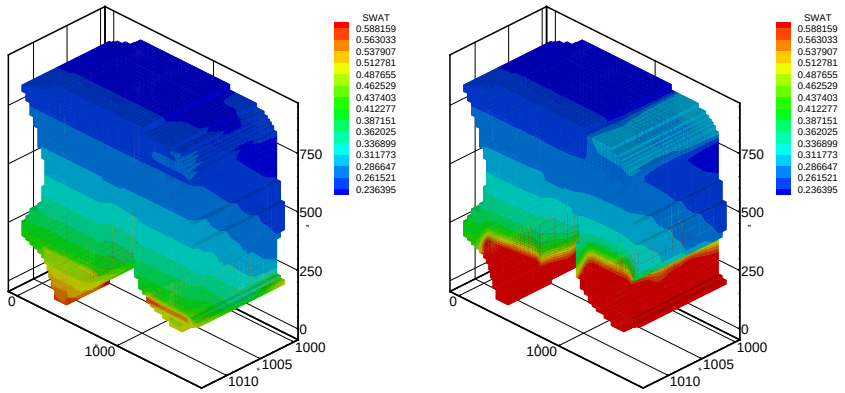

FIGURE 9. Water saturation contours at days 1 and 21

At day 20 of the simulation, we impose a no-flow boundary condition on Γ_1 and Γ_2. Then, after 40 days, we impose a flux condition on Γ_3, so that

$$U_w \cdot \eta|_{\Gamma 3} = 50 \text{ and } U_n \cdot \eta|_{\Gamma 3} = 0,$$

and we impose a Dirichlet condition on the non-wetting phase pressure, but we take the saturation value for the non-wetting phase from the neighboring cell. Thus at day 40 on Γ_4 we set

$$P_n|_{\Gamma_4} = 400,$$

and allow the saturation value to be determined during the computation. This change in boundary conditions can be seen in the transition in water saturation profiles given in Figure 10.

The water saturation and non-wetting phase pressure contours at the end of the simulation are given in Figure 11. Thus you can see the flow moving from Γ_3 to Γ_4, and the separation in water saturations at the Γ_1 and Γ_2 boundary regions. Thus at the end of the simulation, you can see by

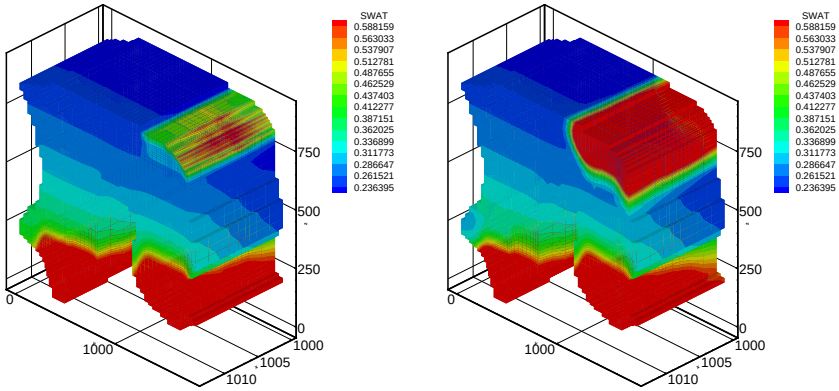

FIGURE 10. Water saturation contours at days 41 and 71

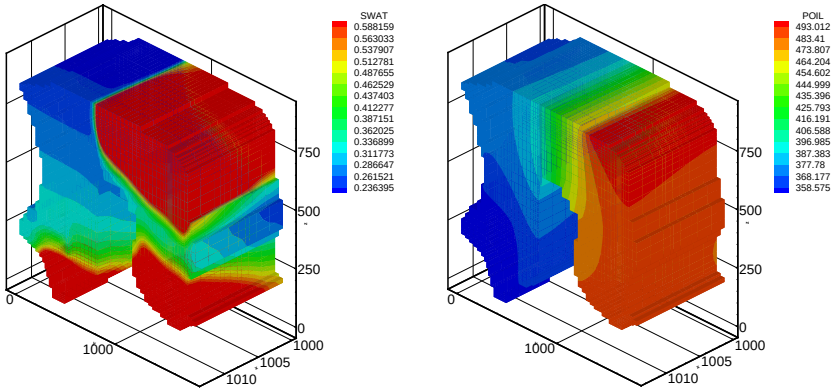

FIGURE 11. Water saturation contour and non-wetting phase pressure at day 161

the saturation profile in Figure 12, that the wetting phase fluid has reached the boundary edge and is being removed from the reservoir.

6. Conclusions

We have shown that our discretization of the two-phase flow models allows for a variety of boundary conditions. This gives us flexibility in our modeling capabilities, as these boundary conditions allow us to more easily couple different physical models. Our discretization is also locally mass conservative.

7. Acknowledgements

The authors wish to acknowledge Dr. John Wheeler for his work on the IPARS framework in particular, on the two-phase model, and for suggestions concerning the design of the boundary conditions input capability.

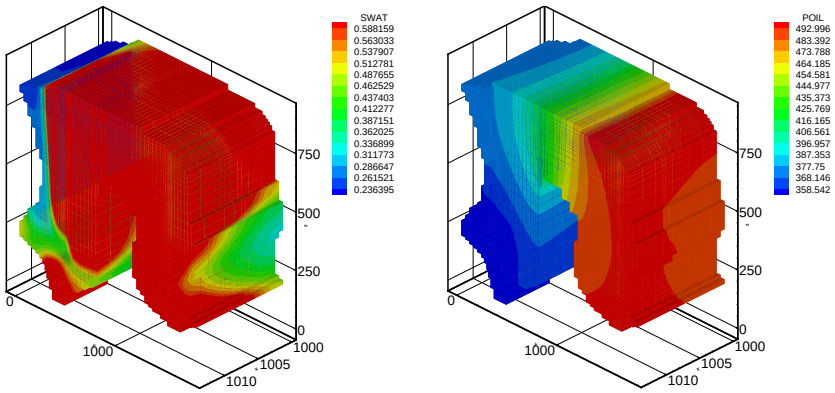

FIGURE 12. Water saturation contour and non-wetting phase pressure at day 451

References

[ABE+] T. Arbogast, S. Bryant, J. Eaton, Q. Lu, M. Peszynska, M. F. Wheeler, and I. Yotov, *A parallel multiblock/multidomain approach for reservoir simulation*, under revision for Society of Petroleum Engineers Journal.

[ACWY00] T. Arbogast, L. C. Cowsar, M. F. Wheeler, and I. Yotov, *Mixed finite element methods on non-matching multiblock grids*, SIAM J. Numer. Anal. **37** (2000), 1295–1315.

[AD85] H. W. Alt and E. DiBenedetto, *Nonsteady flow of water and oil through inhomogeneous porous media*, Ann. Scuola Norm. Sup. Pisa Cl. Sci. **12** (1985), 335–392.

[ADK+98] T. Arbogast, C. N. Dawson, P. T. Keenan, M. F. Wheeler, and I. Yotov, *Enhanced cell-centered finite differences for elliptic equations on general geometry*, SIAM J. Sci. Comp. **19** (1998), no. 2, 404–425.

[Arb92] T. Arbogast, *The existence of weak solutions to single porosity and simple dual-porosity models of two-phase incompressible flow*, Nonlinear Analysis, Theory, Methods and Applications **19** (1992), 1009–1031.

[AS79] K. Aziz and A. Settari, *Petroleum reservoir simulation*, Applied Science, 1979.

[AWY96] T. Arbogast, M. F. Wheeler, and I. Yotov, *Logically rectangular mixed methods for flow in irregular, heterogeneous domains*, Computational Methods in Water Resources XI (A. A. Aldama et al., eds.), Computational Mechanics Publications, Southampton, 1996, pp. 621–628.

[AWY97] ———, *Mixed finite elements for elliptic problems with tensor coefficients as cell-centered finite differences*, SIAM J. Numer. Anal. **34** (1997), no. 2, 828–852.

[AWZ96] Todd Arbogast, Mary F. Wheeler, and Nai-Ying Zhang, *A nonlinear mixed finite element method for a degenerate parabolic equation arising in flow in porous media*, SIAM J. Numer. Anal. **33** (1996), no. 4, 1669–1687.

[BL42] S. E. Buckley and M. C. Leverett, *Mechanism of fluid displacements in sands*, Transactions of the AIME **146** (1942), 107–116.

[Che97] Z. Chen, *On the existence, uniqueness, and regularity of a weak solution to two phase incompressible flow in porous media*, Tech. Report 97-10, Dept. Math., Southern Methodist University, 1997.

[CK01] Zhangxin Chen and Natalia L. Khlopina, *Degenerate two-phase incompressible flow problems. i. regularization and numerical results*, Commun. Appl. Anal. **5** (2001), no. 3, 319–334.

[CQE00] Zhangxin Chen, Guan Qin, and Richard E. Ewing, *Analysis of a compositional model for fluid flow in porous media*, SIAM J. Appl. Math. **60** (2000), no. 3, 747–777 (electronic). MR **2000j:**76134

[DKWW97] C. N. Dawson, H. Klie, M. F. Wheeler, and C. Woodward, *A parallel, implicit, cell-centered method for two-phase flow with a preconditioned Newton-Krylov solver*, Comput. Geosci. **1** (1997), 215–249.

[Eat01] Frank Joseph Eaton, *A multigrid preconditioner for two-phase flow in porous media*, Ph.D. thesis, University of Texas at Austin, December 2001.

[Edw98] H. C. Edwards, *A parallel multilevel-preconditioned GMRES solver for multiphase flow models in the Implicit Parallel Accurate Reservoir Simulator*, Tech. Report 98-04, TICAM, University of Texas at Austin, 1998.

[IPA00] *IPARS User's Manual*, Tech. report, Center for Subsurface Modeling, Texas Institute for Computational and Applied Mathematics, University of Texas at Austin, 1998–2000.

[LNW00] W. Lee, M. Noh, and M. F. Wheeler, *Air-water flow simulation in unsaturated porous media.*, Computational Methods in Water Resources (L. R. Bentley, J. F. Sykes, C. A. Brebbia, W. G. Gray, and G. F. Pinder, eds.), A. A. Balkema, 2000, pp. 93–100.

[LPW01] Q. Lu, M. Peszynska, and M. F. Wheeler, *A parallel multi-block black-oil model in multi-model implementation.*, 2001 SPE Reservoir Simulation Symposium (Houston, Texas), 2001, SPE 66359.

[Lu00] Qin Lu, *A parallel multi-block / multi-physics approach for multi-phase flow in porous media*, Ph.D. thesis, University of Texas at Austin, Austin, Texas, 2000.

[LVW] S. Lacroix, Y. Vassilevski, and M. F. Wheeler, *Iterative solvers of the implicit parallel accurate reservoir simulator (IPARS)*, To appear in Numer. Lin. Algebra Appl.

[MSA+99] S. Minkoff, C. M. Stone, J. G. Arguello, S. Bryant, J. Eaton, M. Peszynska, and M. F. Wheeler, *Staggered in time coupling of reservoir flow simulation and geomechanical deformation: Step 1 - one-way coupling*, 1999 SPE Symposium on Reservoir Simulation (Houston, Texas), 1999, SPE 51920.

[Pea83] D. W. Peaceman, *Interpretation of well-block pressure in numerical reservior simulation with non-square grid blocks and anisotropic permeability*, Tran. AIME **275** (1983), 10–22.

[PLW99] M. Peszynska, Q. Lu, and M. F. Wheeler, *Coupling different numerical algorithms for two phase fluid flow.*, MAFELAP Proceedings of Mathematics of Finite Elements and Applications (Uxbridge, U.K.) (J. R. Whiteman, ed.), Brunel University, 1999, pp. 205–214.

[PLW00] ———, *Multiphysics coupling of codes*, Computational Methods in Water Resources (L. R. Bentley, J. F. Sykes, C. A. Brebbia, W. G. Gray, and G. F. Pinder, eds.), A. A. Balkema, 2000, pp. 175–182.

[PWP+97] M. Parashar, J. A. Wheeler, G. Pope, K. Wang, and P. Wang, *A new generation EOS compositional reservoir simulator. part II: Framework and multiprocessing*, Fourteenth SPE Symposium on Reservoir Simulation, Dallas, Texas, Society of Petroleum Engineers, June 1997, pp. 31–38.

[PWY] M. Peszynska, M. F. Wheeler, and I. Yotov, *Mortar upscaling for multiphase flow in porous media*, Computational Geosciences, to appear.

[RW83] T. F. Russell and M. F. Wheeler, *Finite element and finite difference methods for continuous flows in porous media*, The Mathematics of Reservoir Simulation (R. E. Ewing, ed.), SIAM, Philadelphia, 1983, pp. 35–106.

[WAB+99] M. F. Wheeler, T. Arbogast, S. Bryant, J. Eaton, Q. Lu, M. Peszynska, and I. Yotov, *A parallel multiblock/multidomain approach to reservoir simulation*, Fifteenth SPE Symposium on Reservoir Simulation, Houston, Texas, Society of Petroleum Engineers, 1999, SPE 51884, pp. 51–62.

[Whe] John A. Wheeler, *private communications.*

[WPGED00] M. F. Wheeler, M. Peszynska, X. Gai, and O. El-Domeiri, *Modeling subsurface flow on pc cluster*, High Performance Computing (A. Tentner, ed.), SCS, 2000, pp. 318–323.

[WWP00] M. F. Wheeler, J. A. Wheeler, and M. Peszynska, *A distributed computing portal for coupling multi-physics and multiple domains in porous media.*, Computational Methods in Water Resources (L. R. Bentley, J. F. Sykes, C. A. Brebbia, W. G. Gray, and G. F. Pinder, eds.), A. A. Balkema, 2000, pp. 167–174.

[WYW+97] P. Wang, I. Yotov, M. F. Wheeler, T. Arbogast, C. N. Dawson, M. Parashar, and K. Sepehrnoori, *A new generation EOS compositional reservoir simulator. part I: Formulation and discretization*, Fourteenth SPE Symposium on Reservoir Simulation, Dalas, Texas, Society of Petroleum Engineers, June 1997, pp. 55–64.

[Yot96] I. Yotov, *Mixed finite element methods for flow in porous media*, Ph.D. thesis, Rice University, Houston, Texas, 1996, TR96-09, Dept. Comp. Appl. Math., Rice University and TICAM report 96-23, University of Texas at Austin.

Texas Institute for Computational and Applied Mathematics, University of Texas, Austin, TX 78712 U.S.A.

E-mail address: mpesz@ticam.utexas.edu, lea@ticam.utexas.edu, mfw@ticam.utexas.edu